Available online at www.sciencedirect.com
SCIENCE DIRECT®
Journal of Sound and Vibration 288 (2005) 887–906
JOURNAL OF SOUND AND VIBRATION
www.elsevier.com/locate/jsvi

Analytical and differential quadrature results for vibration analysis of damaged circular arches

Erasmo Viola*, Edoardo Artioli, Michele Dilena

DISTART, Department of Structural Engineering, University of Bologna, V.le Risorgimento 2, I-40136 Bologna, Italy

Received 24 November 2003; received in revised form 7 December 2004; accepted 13 January 2005
Available online 9 April 2005

Abstract

The present paper focuses on in-plane linear free vibrations of circular arches, in undamaged and damaged configurations. For the model herein utilized, the equations of motion, in terms of displacements and rotation, take into account shearing and axial deformations and rotary inertia. The cracked section of the arch is modeled with an elastic spring. An exact analytical method of solution and an approximate numerical one are presented. The first method solves the fundamental system in closed form, by means of a characteristic polynomial; the second one is based on a simple and efficient differential quadrature and domain decomposition technique. Natural frequencies and mode shapes are computed for some significant cases, showing very good agreement between the two approaches.

1. Introduction

Due to its theoretical and practical importance, the free in-plane vibration problem of arches and rings has become a widely investigated field and a number of publications on this subject is available in the scientific literature. The first studies on this argument date back to the work of Lamb [1], Love [2] and Den Hartog [3] and frequently still appeared in the scientific literature. The available general complete structural models, in the arch case, become complicated due to the

*Corresponding author. Tel.: +39 051 209 3510; fax: +39 051 209 3496.
E-mail address: erasmo.viola@mail.ing.unibo.it (E. Viola).

0022-460X/$ - see front matter © 2005 Elsevier Ltd. All rights reserved.
doi:10.1016/j.jsv.2005.01.027

curvilinear geometry, which produces a coupling between displacements and rotation in the equations of motion. However, the problem can be somewhat simplified, introducing certain assumptions on the kinematic assessment of the arch and on its inertial properties. Among the simplified models available in the open literature, we mention the one with negligible rotary inertia, shearing deformation and axial extensibility [4,5], which gives a singular sixth-order partial differential equation of motion; and the model which accounts for axial deformability but not for rotational inertia and for transverse deformations [6,7], governed by two coupled differential equations for the tangential and radial displacements. Finally, one has the "complete" model which takes into account the total of these three contributions and is governed by a triplet of coupled second-order differential equations for the unknown rotation and displacements [8,9]. With regard to this complete model, different solving approaches have been proposed. For example, Tüfekçi and Arpaci [8] solved the free harmonic vibration problem for the circular uniform arch with several boundary conditions. Irie et al. [10] applied the transfer matrix method in the in-plane vibrations analysis of circular arches with different sections and different sets of boundary conditions. An hybrid-mixed element was proposed by Benedetti et al. [11], for the case of a general curvilinear arch structure with variable cross section and curvature along the axis, based on a modified formulation of the Hellinger–Reissner principle, while Tseng et al. [12] introduce the dynamic stiffness method for the in-plane vibrations of general curvilinear compound with variable curvature. Recently, Wu and Chiang [9] utilized a circular arch finite element with two nodes and 6 dof.

The numerous previous studies are focused on the dynamic behavior of the arch in the undamaged configuration. Even if, for the case of straight beams with a localized damage, many reports are available in the literature, see, for example, Refs. [13–15], the same does not hold true for the arch and to the very best of the authors' knowledge, minor attention has been given to the analysis of such structures in damaged configuration [16,17]. The goal of this paper, thus, is to provide a contribution in this direction and to investigate the free harmonic vibration problem of circular arches, modelling the cracked cross section with an elastic hinge [18–21]. For each arch segment generated by the crack, the equations of motion have been written with no simplifying hypothesis. Once the boundary conditions and jump conditions across the damaged section have been set, the solution of the problem, in terms of natural frequencies and mode shapes, has been obtained.

The first strategy adopted herein is an analytical one and is based on roots finding of the characteristic polynomial. The second method, a numerical one known as Differential Quadrature (D.Q.) method [22], has been tested for computational efficiency and validated by comparison with analytical results. A similar collocation method had already been applied to the linear vibration and stability analysis of straight and curved beams by Kang et al. [23,24] in a slightly different form from the one adopted in the present work. The D.Q. method permits to discretize both the governing equations and boundary conditions, together with the jump conditions [25–27], avoiding any simplifying hypothesis in the physical model such as the so called δ-point technique [28]. The polynomial interpolation rule for the configuration variables provides clearly accurate results for the examined modal parameters and the corresponding quadrature formulas can be derived in a simple recursive manner, once the collocation points are chosen on the domain [29].

Accordingly, the first fundamental frequencies for a couple of specimen structures both in undamaged and damaged configurations have been computed, for different locations and severity of the crack.

In all the examined cases an optimal agreement can be observed between results obtained using the two procedures. The frequency variations depend both on position and severity of the damage and surely can constitute a good efficiency state indicator for the considered arch. Possible future developments of the proposed approaches could be the crack identification problem by eigenparameters variations between damaged and undamaged configurations and the analysis of the dynamic behavior of the arch when material and geometric nonlinearities are considered.

2. Statement of the problem

Let us consider a uniform circular arch, as shown in Fig. 1, with different boundary conditions. Let us suppose that the system vibrates freely in the vertical plane, with small oscillations around a circular and unstressed configuration of equilibrium. The kinematics of the arch is thoroughly defined by assigning the tangential displacement $u(\theta, t)$, the normal displacement $v(\theta, t)$ and the rotation angle about the binormal axis $\varphi(\theta, t)$ of the θ angular coordinate cross section at a moment of time t.

Taking into account the effect of shear and axial deformations and rotary inertia, the equations of motion can be written as follows (see Refs. [8,30])

$$\frac{1}{R}\frac{\partial N(\theta,t)}{\partial\theta} - \frac{V(\theta,t)}{R} = \rho A\,\frac{\partial^2 u(\theta,t)}{\partial t^2},$$

$$\frac{1}{R}\frac{\partial V(\theta,t)}{\partial\theta} + \frac{N(\theta,t)}{R} = \rho A\,\frac{\partial^2 v(\theta,t)}{\partial t^2},$$

$$\frac{1}{R}\frac{\partial M(\theta,t)}{\partial\theta} - V(\theta,t) = \rho I\,\frac{\partial^2 \varphi(\theta,t)}{\partial t^2}, \tag{1}$$

for $\theta \in (-\Theta, \Theta)$, and $t > 0$. In the previous equations, $N(\theta, t)$, $V(\theta, t)$ and $M(\theta, t)$, denote the axial force, the shearing force and the bending moment, respectively. Moreover, R is the radius of the

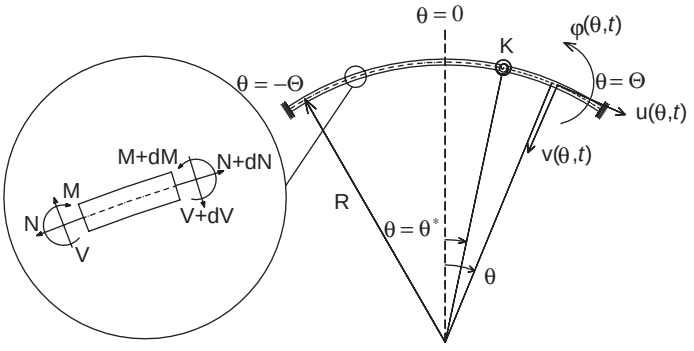

Fig. 1. Clamped–clamped circular arch with indication of damage position.

arch, ρ is the mass density for unit volume, A and I are the area and the moment of inertia of the transversal section. The internal forces can be expressed by the constitutive relations

$$N(\theta,t)=\frac{EA}{R}\left(\frac{\partial u(\theta,t)}{\partial\theta}-v(\theta,t)\right),$$

$$V(\theta,t)=\frac{GA}{R\chi}\left(u(\theta,t)+\frac{\partial v(\theta,t)}{\partial\theta}+R\varphi(\theta,t)\right),$$

$$M(\theta,t)=\frac{EI}{R}\frac{\partial\varphi(\theta,t)}{\partial\theta}, \tag{2}$$

where E, G are Young's and shear moduli, χ is the shear factor.

We suppose now that a crack appears at the cross section of angular coordinate $\theta^*\in(-\Theta,\Theta)$; if the crack remains always open during the vibration of the arch, it can be modeled as a massless rotational elastic spring at the damaged cross section, see Refs. [19–21]. The stiffness K of the spring can be related in a precise way to the geometry of damage, as suggested, for example, by Dimarogonas and Paipetis [31].

Substituting relations (2) in Eq. (1), the equations of motion can be written separately in the two intervals $(-\Theta,\theta^*)$ and (θ^*,Θ), in terms of displacements components only

$$\frac{EA}{R^2}\frac{\partial}{\partial\theta}\left(\frac{\partial u^{(\alpha)}(\theta,t)}{\partial\theta}-v^{(\alpha)}(\theta,t)\right)-\frac{GA}{R^2\chi}\left(u^{(\alpha)}(\theta,t)+\frac{\partial v^{(\alpha)}(\theta,t)}{\partial\theta}+R\varphi^{(\alpha)}(\theta,t)\right)=\rho A\frac{\partial^2u^{(\alpha)}(\theta,t)}{\partial t^2},$$

$$\frac{GA}{R^2\chi}\frac{\partial}{\partial\theta}\left(u^{(\alpha)}(\theta,t)+\frac{\partial v^{(\alpha)}(\theta,t)}{\partial\theta}+R\varphi^{(\alpha)}(\theta,t)\right)+\frac{EA}{R^2}\left(\frac{\partial u^{(\alpha)}(\theta,t)}{\partial\theta}-v^{(\alpha)}(\theta,t)\right)=\rho A\frac{\partial^2v^{(\alpha)}(\theta,t)}{\partial t^2},$$

$$\frac{EI}{R^2}\frac{\partial^2\varphi^{(\alpha)}(\theta,t)}{\partial\theta^2}-\frac{GA}{R\chi}\left(u^{(\alpha)}(\theta,t)+\frac{\partial v^{(\alpha)}(\theta,t)}{\partial\theta}+R\varphi^{(\alpha)}(\theta,t)\right)=\rho I\frac{\partial^2\varphi^{(\alpha)}(\theta,t)}{\partial t^2}, \tag{3}$$

for $\alpha=1,2$. In the previous equations the indices $\alpha=1,2$ denote the left and right segment of the arch, respectively $(-\Theta,\theta^*)$ and (θ^*,Θ). Eqs. (3) show that the small vibrations of the circular cracked arch are regulated by a system of six differential equations, three per each segment individuated by the crack, where a coupling takes place between tangential displacement $(u^{(\alpha)}(\theta,t))$, normal displacement $(v^{(\alpha)}(\theta,t))$ and rotation $(\varphi^{(\alpha)}(\theta,t))$. A proper set of boundary conditions must be adjoined, as follows

(i) *Clamped–clamped*:

$$u^{(1)}(-\Theta,t)=u^{(2)}(\Theta,t)=0,$$

$$v^{(1)}(-\Theta,t)=v^{(2)}(\Theta,t)=0,\quad t>0,$$

$$\varphi^{(1)}(-\Theta,t)=\varphi^{(2)}(\Theta,t)=0. \tag{4}$$

(ii) *Hinged–hinged*:

$$u^{(1)}(-\Theta,t)=u^{(2)}(\Theta,t)=0,$$

$$v^{(1)}(-\Theta,t)=v^{(2)}(\Theta,t)=0,\quad t>0,$$

$$M^{(1)}(-\Theta,t)=M^{(2)}(\Theta,t)=0. \tag{5}$$

(iii) *Free–free*:

$$N^{(1)}(-\Theta,t)=N^{(2)}(\Theta,t)=0,$$

$$V^{(1)}(-\Theta,t)=V^{(2)}(\Theta,t)=0,\quad t>0,$$

$$M^{(1)}(-\Theta,t)=M^{(2)}(\Theta,t)=0 \tag{6}$$

just as the following jump conditions

$$u^{(2)}(\theta^*,t)-u^{(1)}(\theta^*,t)=0,$$

$$v^{(2)}(\theta^*,t)-v^{(1)}(\theta^*,t)=0,$$

$$K(\varphi^{(2)}(\theta^*,t)-\varphi^{(1)}(\theta^*,t))=M^{(1)}(\theta^*,t),$$

$$N^{(2)}(\theta^*,t)-N^{(1)}(\theta^*,t)=0,\quad t>0,$$

$$V^{(2)}(\theta^*,t)-V^{(1)}(\theta^*,t)=0,$$

$$M^{(2)}(\theta^*,t)-M^{(1)}(\theta^*,t)=0 \tag{7}$$

hold at the cross section where the crack occurs. The undamaged arch corresponds to $K\to\infty$, or, equivalently, to $\varphi^{(2)}(\theta^*,t)-\varphi^{(1)}(\theta^*,t)=0$.

In the following section the case of an arch in undamaged and damaged configuration, having constant elastic and inertial properties, will be closely examined.

3. Analytical and numerical solutions

3.1. Exact solution

The free undamped vibrations of an uniform arch in damaged configuration are regulated by the coupled system of partial differential equations (3), with the suitable boundary conditions (4)–(6) in the case of clamped, hinged or free ends, respectively, and jump conditions (7). We seek solutions that are harmonic in time and whose frequency is ω; then, the displacements and the rotation angle can be written as

$$u^{(\alpha)}(\theta,t)=u^{(\alpha)}(\theta)\cos\omega t,$$

$$v^{(\alpha)}(\theta,t)=v^{(\alpha)}(\theta)\cos\omega t,$$

$$\varphi^{(\alpha)}(\theta,t)=\varphi^{(\alpha)}(\theta)\cos\omega t, \tag{8}$$

where the vibration spatial amplitude values ($u^{(\alpha)}(\theta)$, $v^{(\alpha)}(\theta)$, $\varphi^{(\alpha)}(\theta)$) fulfill the differential system

$$EA\frac{\mathrm{d}}{\mathrm{d}\theta}\left(\frac{\mathrm{d}u^{(\alpha)}(\theta)}{\mathrm{d}\theta}-v^{(\alpha)}(\theta)\right)-\frac{GA}{\chi}\left(u^{(\alpha)}(\theta)+\frac{\mathrm{d}v^{(\alpha)}(\theta)}{\mathrm{d}\theta}+R\varphi^{(\alpha)}(\theta)\right)+\omega^2R^2\rho Au^{(\alpha)}(\theta)=0,$$

$$\frac{GA}{\chi}\frac{\mathrm{d}}{\mathrm{d}\theta}\left(u^{(\alpha)}(\theta)+\frac{\mathrm{d}v^{(\alpha)}(\theta)}{\mathrm{d}\theta}+R\varphi^{(\alpha)}(\theta)\right)+EA\left(\frac{\mathrm{d}u^{(\alpha)}(\theta)}{\mathrm{d}\theta}-v^{(\alpha)}(\theta)\right)+\omega^2R^2\rho Av^{(\alpha)}(\theta)=0,$$

$$EI\frac{\mathrm{d}^2\varphi^{(\alpha)}(\theta)}{\mathrm{d}\theta^2}-\frac{GAR}{\chi}\left(u^{(\alpha)}(\theta)+\frac{\mathrm{d}v^{(\alpha)}(\theta)}{\mathrm{d}\theta}+R\varphi^{(\alpha)}(\theta)\right)+\omega^2R^2\rho I\varphi^{(\alpha)}(\theta)=0, \tag{9}$$

for $\alpha=1,2$.

The six boundary conditions are expressed as

(i) *Clamped–clamped*:

$$u^{(1)}(-\Theta)=u^{(2)}(\Theta)=0,$$

$$v^{(1)}(-\Theta)=v^{(2)}(\Theta)=0,$$

$$\varphi^{(1)}(-\Theta)=\varphi^{(2)}(\Theta)=0. \tag{10}$$

(ii) *Hinged–hinged*:

$$u^{(1)}(-\Theta)=u^{(2)}(\Theta)=0,$$

$$v^{(1)}(-\Theta)=v^{(2)}(\Theta)=0,$$

$$\frac{\mathrm{d}\varphi^{(1)}(-\Theta)}{\mathrm{d}\theta}=\frac{\mathrm{d}\varphi^{(2)}(\Theta)}{\mathrm{d}\theta}=0. \tag{11}$$

(iii) *Free–free*:

$$\frac{\mathrm{d}u^{(1)}(-\Theta)}{\mathrm{d}\theta}-v^{(1)}(-\Theta)=\frac{\mathrm{d}u^{(2)}(\Theta)}{\mathrm{d}\theta}-v^{(2)}(\Theta)=0,$$

$$u^{(1)}(-\Theta)+\frac{\mathrm{d}v^{(1)}(-\Theta)}{\mathrm{d}\theta}+R\varphi^{(1)}(-\Theta)=u^{(2)}(\Theta)+\frac{\mathrm{d}v^{(2)}(\Theta)}{\mathrm{d}\theta}+R\varphi^{(2)}(\Theta)=0,$$

$$\frac{\mathrm{d}\varphi^{(1)}(-\Theta)}{\mathrm{d}\theta}=\frac{\mathrm{d}\varphi^{(2)}(\Theta)}{\mathrm{d}\theta}=0, \tag{12}$$

and the six jump conditions

$$u^{(2)}(\theta^*) - u^{(1)}(\theta^*) = 0,$$

$$v^{(2)}(\theta^*) - v^{(1)}(\theta^*) = 0,$$

$$K(\varphi^{(2)}(\theta^*) - \varphi^{(1)}(\theta^*)) = \frac{EI}{R}\frac{\mathrm{d}\varphi^{(1)}(\theta^*)}{\mathrm{d}\theta},$$

$$\frac{\mathrm{d}u^{(2)}(\theta^*)}{\mathrm{d}\theta} - v^{(2)}(\theta^*) - \frac{\mathrm{d}u^{(1)}(\theta^*)}{\mathrm{d}\theta} + v^{(1)}(\theta^*) = 0,$$

$$u^{(2)}(\theta^*) + \frac{\mathrm{d}v^{(2)}(\theta^*)}{\mathrm{d}\theta} + R\varphi^{(2)}(\theta^*) - u^{(1)}(\theta^*) - \frac{\mathrm{d}v^{(1)}(\theta^*)}{\mathrm{d}\theta} - R\varphi^{(1)}(\theta^*) = 0,$$

$$\frac{\mathrm{d}\varphi^{(2)}(\theta^*)}{\mathrm{d}\theta} - \frac{\mathrm{d}\varphi^{(1)}(\theta^*)}{\mathrm{d}\theta} = 0, \tag{13}$$

for $t>0$. The complete primitive $(u^{(\alpha)}(\theta), v^{(\alpha)}(\theta), \varphi^{(\alpha)}(\theta))$ of system (9) takes the form of

$$(u^{(\alpha)}(\theta), v^{(\alpha)}(\theta), \varphi^{(\alpha)}(\theta)) = \sum_{\beta=1}^{6} c_\beta^{(\alpha)}(w_1^{(\alpha)}, w_2^{(\alpha)}, w_3^{(\alpha)})^{(\beta)} \exp(\lambda_\beta^{(\alpha)}\theta), \tag{14}$$

for $\alpha = 1, 2$, where $\{c_\beta^{(\alpha)}\}_{\beta=1}^6$ is a vector of unknowns constants which depend on the boundary conditions. In Eq. (14), $\{\lambda_\beta^{(\alpha)}, \mathbf{w}^{(\alpha,\beta)} \equiv (w_1^{(\alpha)}, w_2^{(\alpha)}, w_3^{(\alpha)})^{(\beta)}\}$ is the βth eigenpair of the eigenvalue problem in the θ spatial variable for the αth interval of the arch. Applying the Euler characteristic exponents method, we seek solutions for system (9) having the form of $\exp(\lambda_\beta^{(\alpha)}\theta)\mathbf{w}^{(\alpha,\beta)}$.

The 12 complex numbers $\{\lambda_\beta^{(\alpha)}\}_{\beta=1}^6$ are the roots of the characteristic polynomials

$$p^{(\alpha)}(\lambda) = d_0 + d_1(\lambda^{(\alpha)})^2 + d_2(\lambda^{(\alpha)})^4 + d_3(\lambda^{(\alpha)})^6, \tag{15}$$

where

$$d_0 = EA\frac{GA}{\chi}(AR^2 + I)\Omega - \left[EAI + \frac{GA}{\chi}(AR^2 + I)\right]A\Omega^2 + A^2I\Omega^3,$$

$$d_1 = EA\frac{GA}{\chi}EI - \left[EA\frac{GA}{\chi}(AR^2 - 2I) + EIA\left(EA + \frac{GA}{\chi}\right)\right]\Omega + \left(2EA + \frac{GA}{\chi}\right)AI\Omega^2,$$

$$d_2 = 2EA\frac{GA}{\chi}EI + \left(EA + 2\frac{GA}{\chi}\right)EAI\Omega,$$

$$d_3 = EA\frac{GA}{\chi}EI, \tag{16}$$

and $\Omega \equiv \omega^2\rho R^2$. A parametric study of the roots of polynomials $p^{(\alpha)}(\lambda^{(\alpha)})$ shows that the roots $(\lambda^{(\alpha)})^2$ can be real value (positive or negative) or complex value functions of frequency ω. This fact allows the representation of the exponential factors present in expressions (14) through harmonic functions if $(\lambda^{(\alpha)})^2$ root of $p^{(\alpha)}(\lambda^{(\alpha)})$ is negative, through hyperbolic functions if $(\lambda^{(\alpha)})^2$ is positive,

and through a suitable combination of products of harmonic and hyperbolic functions if $(\lambda^{(\alpha)})^2$ root of $p^{(\alpha)}(\lambda^{(\alpha)})$ is complex.

Considering that the $\mathbf{w}^{(\alpha,\beta)}$ eigenvector, with $\beta = 1,\ldots,6$, is proportional to the vector of components

$$w_1 = 1,$$

$$w_2(\lambda_\beta^{(\alpha)}) = -\frac{\lambda_\beta^{(\alpha)}[EA((\lambda_\beta^{(\alpha)})^2+1)+A\Omega]}{A\Omega - EA((\lambda_\beta^{(\alpha)})^2+1)},$$

$$w_3(\lambda_\beta^{(\alpha)}) = \frac{\chi}{GAR}\left[\left(EA(\lambda_\beta^{(\alpha)})^2 - \frac{GA}{\chi} + A\Omega\right) - \lambda_\beta^{(\alpha)}\left(EA + \frac{GA}{\chi}\right)w_2(\lambda_\beta^{(\alpha)})\right], \tag{17}$$

the characteristic polynomial can be then formed for the eigenvalue problem (9), by imposing that the general solution (14) must fulfill boundary conditions (10), (11) or (12) and the jump conditions (13). In so doing, one obtains a homogeneous linear system in real constants $\mathbf{c} = \{c_\beta^{(\alpha)}\}_{\beta=1}^6$, for example, $\mathbf{M}(\omega)\mathbf{c} = \mathbf{0}$, where $\mathbf{M}(\omega)$ is a 12×12 matrix depending on ω. Natural cyclic pulsations correspond to those special ω values that cancel out the determinant of $\mathbf{M}(\omega)$. In order to determine the natural pulsations of the arch as roots of the characteristic polynomial $\det \mathbf{M}(\omega)$, a numeric procedure was adopted, whose essential steps can be summarized as follows. Once a value for ω was set, say ω^*, the sixth degree polynomial equations in $\lambda^{(\alpha)}$, $p^{(\alpha)}(\lambda^{(\omega)}) = 0$, were solved, $\alpha = 1, 2$, where $p^{(\alpha)}(\lambda^{(\alpha)})$ were assumed like in expression (15). Once the six $\lambda^{(\alpha)}$ roots of $p^{(\alpha)}(\lambda^{(\alpha)})$ were found, the expressions of the eigensolutions $\exp(\lambda^{(\alpha)}\theta)\mathbf{w}^{(\alpha,\beta)}$ were determined by imposing the proper conditions at both ends of the arch and at the damaged cross section, as well as the value of $\det \mathbf{M}(\omega^*)$. By repeating this procedure for $\omega^* + \Delta\omega$, where $\Delta\omega$ is a small increment, the graph of $\det \mathbf{M}(\omega)$ was reconstructed in a given frequency range. Eigenfrequency values were calculated by a false position method applied between the two values of the ω variable, corresponding to a change of sign of $\det \mathbf{M}(\omega)$. For each eigenfrequency value, after solving $\mathbf{Mc} = \mathbf{0}$, the vector $\mathbf{c}$ was calculated and therefore the corresponding mode of vibration was determined.

3.2. D.Q. solution

A novel approach in numerically solving the governing equations (9) is represented by the D.Q. method, coupled with a proper domain decomposition technique [24–26,32], necessary to enforce the jump conditions across the cracked section. This method pertains to the class of collocation methods and, for the problem studied herein, demonstrates its numerical accuracy and extreme coding simplicity. The basic steps in the D.Q. solution of the free vibration problem of damaged circular arches are as follows [29]:

- A discretization of independent (space) variable $\theta \in [-\Theta, \Theta]$ into each subdomain $\alpha = 1, 2$ by a suitable number of collocation points $\theta_i^{(1)} \in \{\theta_1^{(1)}, \theta_2^{(1)}, \ldots, \theta_m^{(1)}\}$, $\theta_i^{(2)} \in \{\theta_1^{(2)}, \theta_2^{(2)}, \ldots, \theta_n^{(2)}\}$, is made by taking into account the domain decomposition due to the two arch segments.
- An interpolation of dependent variables $(u^{(\alpha)}(\theta^{(\alpha)}), v^{(\alpha)}(\theta^{(\alpha)}), \varphi^{(\alpha)}(\theta^{(\alpha)}))$ through local values in the collocation points of each subdomain is performed.

- The spatial derivatives are approximated according to the previous interpolation rule.
- The differential governing systems (9) are transformed into linear eigenvalue problems for the natural frequencies; the boundary and the jump conditions being imposed in the collocation points corresponding to the boundary and the cracking nodes. All these relations are imposed pointwise.
- The solution of the previously stated discrete system in terms of natural frequencies and mode shapes components is worked out. For each mode, using the aforementioned interpolation, local values of dependent variables are used to obtain the complete assessment of deformed configuration. The approximated states of stress and deformation can be obtained by using the corresponding relationships.

In what precedes there are two basic choices left arbitrary, i.e. the collocation points and the interpolation scheme adopted. In the present study, Lagrange interpolating polynomials will be used coupled with a rational sampling of grid points [33], along the two segments of the circular arch.

In what follows a hint to the discretization of governing differential equation will be given; for example, the tangential displacement $u^{(\alpha)}$ is approximated as

$$u^{(\alpha)} = \sum_{i=1}^{m,n} L_i(\theta^{(\alpha)}) u^{(\alpha)}(\theta_i^{(\alpha)}) = \sum_{i=1}^{m,n} L_i^{(\alpha)} u_i^{(\alpha)}, \quad i = 1, \ldots, m/n, \quad \alpha = 1, 2, \tag{18}$$

where $L_i^{(\alpha)}$ are common Lagrange polynomials, depending on each collocation grid. Accordingly, the spatial derivative of this displacement, evaluated at a certain node $\theta_i^{(\alpha)}$, takes the following form:

$$\left.\frac{\mathrm{d}^r u^{(\alpha)}}{\mathrm{d}\theta^{(\alpha)^r}}\right|_{\theta_i^{(\alpha)}} = \sum_{k=1}^{m,n} a_{ik}^{(\alpha)r} u_k^{(\alpha)}, \quad i = 1, \ldots, m/n, \quad \alpha = 1, 2 \ldots. \tag{19}$$

The preceding coefficients $a_{ik}^{(\alpha)r}$ are known as *weighting coefficients* and are dependent on the derivative order r, on the collocation points $\theta_k^{(\alpha)}$ and on the specific point $\theta_i^{(\alpha)}$, where the derivative is computed. A simple and recursive relationship for the kind of interpolation used has been obtained [33]

$$a_{ik}^{(\alpha)r} = \frac{\prod(\theta_k^{(\alpha)})}{(\theta_i^{(\alpha)} - \theta_k^{(\alpha)}) \prod(\theta_i^{(\alpha)})}, \quad a_{ii}^{(\alpha)r} = \sum_{k \neq i} \frac{1}{(\theta_i^{(\alpha)} - \theta_k^{(\alpha)})}, \quad i = 1, \ldots, m/n, \tag{20}$$

where

$$\prod(\theta_k^{(\alpha)}) = \prod_{p \neq k} (\theta_k^{(\alpha)} - \theta_p^{(\alpha)}). \tag{21}$$

Higher-order coefficients can be found using the following formula:

$$a_{ik}^{(\alpha)r+1} = r\left(a_{ik}^{(\alpha)1} a_{ik}^{(\alpha)r} + \frac{a_{ik}^{(\alpha)r-1}}{(\theta_i^{(\alpha)} - \theta_k^{(\alpha)})}\right), \quad a_{ii}^{(\alpha)r+1} = -\sum_{k \neq i} a_{ik}^{(\alpha)r+1}, \quad i = 1, \ldots, m/n, \tag{22}$$

Last, the choice of sampling points must be made. With Lagrange interpolating polynomials, Chebyshev–Gauss–Lobatto sampling points rule proves efficient for numerical reasons [32] in a way that for such a collocation the approximation error of dependent variable decreases as the number of nodes increases. Moreover, when compared with different quadrature techniques, it provides a less-expensive computation effort in calculating the weighting coefficients and a sufficiently accurate representation of approximated displacements. Accordingly, each collocation will be of the form

$$\theta_i^{(1)} = -\Theta + (\theta^* + \Theta)\,\frac{1}{2}\left(1 - \cos\frac{\pi(i-1)}{m-1}\right), \quad i = 1,\ldots,m,$$

$$\theta_i^{(2)} = \theta^* + (\Theta - \theta^*)\,\frac{1}{2}\left(1 - \cos\frac{\pi(i-1)}{n-1}\right), \quad i = 1,\ldots,n. \tag{23}$$

The simple numerical operations just illustrated, enable to write the equations of motion in discrete form, transforming any space derivative in a weighted sum of node values of dependent variables. Each triplet of approximated equations is valid in a single collocation point belonging to one of the two arch segments. For the left segment, for example, one has

$$EA\left(\sum_{k=1}^{m} a_{ik}^{(1)2} u_k^{(1)} - \sum_{k=1}^{m} a_{ik}^{(1)1} v_k^{(1)}\right) - \frac{GA}{\chi}\left(u_i^{(1)} + \sum_{k=1}^{m} a_{ik}^{(1)1} v_k^{(1)} + R\varphi_i^{(1)}\right) + \omega^2 R^2 \rho A u_i^{(1)} = 0,$$

$$\frac{GA}{\chi}\left(\sum_{k=1}^{m} a_{ik}^{(1)1} u_k^{(1)} + \sum_{k=1}^{m} a_{ik}^{(1)2} v_k^{(1)} + R\sum_{k=1}^{m} a_{ik}^{(1)1} \varphi_k^{(1)}\right) + EA\left(\sum_{k=1}^{m} a_{ik}^{(1)1} u_k^{(1)} - v_i^{(1)}\right) + \omega^2 R^2 \rho A v_i^{(1)} = 0,$$

$$EI\sum_{k=1}^{m} a_{ik}^{(1)2} \varphi_k^{(1)} - \frac{GAR}{\chi}\left(u_i^{(1)} + \sum_{k=1}^{m} a_{ik}^{(1)1} v_k^{(1)} + R\varphi_i^{(1)}\right) + \omega^2 R^2 \rho I \varphi_i^{(1)} = 0, \tag{24}$$

$i = 2,\ldots,m-1$, and the sets of boundary conditions, that need to be imposed in the left extreme point $\theta_1^{(1)}$:

(i) *Clamped*:

$$u_1^{(1)} = 0,$$

$$v_1^{(1)} = 0,$$

$$\varphi_1^{(1)} = 0. \tag{25}$$

(ii) *Hinged*:

$$u_1^{(1)} = 0,$$

$$v_1^{(1)} = 0,$$

$$\sum_{k=1}^{m} a_{1k}^{(1)1}\varphi_k^{(1)} = 0. \tag{26}$$

(iii) *Free*:

$$\sum_{k=1}^{m} a_{1k}^{(1)1}u_k^{(1)} - v_1^{(1)} = 0,$$

$$u_1^{(1)} + \sum_{k=1}^{m} a_{1k}^{(1)1}v_k^{(1)} + R\varphi_1^{(1)} = 0,$$

$$\sum_{k=1}^{m} a_{1k}^{(1)1}\varphi_k^{(1)} = 0. \tag{27}$$

For the right segment similar approximated equations, by means of the above differential quadrature rule, can be set. In correspondence of the crack (left segment last node/right segment first node) the counterpart of the jump conditions (13) must be imposed by means of the D.Q.:

$$u_m^{(1)} = u_1^{(2)},$$

$$v_m^{(1)} = v_1^{(2)},$$

$$K(\varphi_1^{(2)} - \varphi_m^{(1)}) = \frac{EI}{R}\sum_{k=1}^{m} a_{mk}^{(1)1}\varphi_k^{(1)} \quad \left(\text{or} = \frac{EI}{R}\sum_{k=1}^{n} a_{1k}^{(2)1}\varphi_k^{(2)}\right),$$

$$\sum_{k=1}^{n} a_{1k}^{(2)1}u_k^{(2)} - v_1^{(2)} = \sum_{k=1}^{m} a_{mk}^{(1)1}u_k^{(1)} - v_m^{(1)},$$

$$u_1^{(2)} + \sum_{k=1}^{n} a_{1k}^{(2)2}v_k^{(2)} + R\varphi^{(2)}(\theta^*) = u_m^{(1)} + \sum_{k=1}^{m} a_{mk}^{(1)2}v_k^{(1)} + R\varphi_m^{(1)},$$

$$\sum_{k=1}^{n} a_{1k}^{(2)1}\varphi_k^{(2)} = \sum_{k=1}^{m} a_{mk}^{(1)1}\varphi_k^{(1)}. \tag{28}$$

A similar triplet of (domain, boundary, jump) conditions can be easily written for the right part of the arch delimited by the crack, the jump conditions remaining the same in both cases. Now, applying the differential quadrature procedure, the whole system of differential equations can be discretized and the global assembling leads to the following set of linear algebraic equations:

$$\mathbf{K}\boldsymbol{\delta} = \omega^2\mathbf{M}\boldsymbol{\delta}, \tag{29}$$

where, the global stiffness matrix has the following structure:

$$\mathbf{K} = \begin{bmatrix} \underset{3\times3}{\mathbf{K}^{(1)}_{bb}} & \underset{3\times3}{\mathbf{K}^{(1)}_{bc}} & \mathbf{0} & \mathbf{0} & \underset{3\times(m-2)}{\mathbf{K}^{(1)}_{bd}} & \mathbf{0} \\ \underset{3\times3}{\mathbf{K}^{(1)}_{cb}} & \underset{3\times3}{\mathbf{K}^{(1)}_{cc}} & \mathbf{0} & \mathbf{0} & \underset{3\times(n-2)}{\mathbf{K}^{(1)}_{cd}} & \mathbf{0} \\ \mathbf{0} & \mathbf{0} & \underset{3\times3}{\mathbf{K}^{(2)}_{cc}} & \underset{3\times3}{\mathbf{K}^{(2)}_{cb}} & \mathbf{0} & \underset{3\times(m-2)}{\mathbf{K}^{(2)}_{cd}} \\ \mathbf{0} & \mathbf{0} & \underset{3\times3}{\mathbf{K}^{(2)}_{bc}} & \underset{3\times3}{\mathbf{K}^{(2)}_{bb}} & \mathbf{0} & \underset{3\times(n-2)}{\mathbf{K}^{(2)}_{bd}} \\ \underset{(m-2)\times3}{\mathbf{K}^{(1)}_{db}} & \underset{(n-2)\times3}{\mathbf{K}^{(1)}_{dc}} & \mathbf{0} & \mathbf{0} & \underset{3(m-2)\times3(m-2)}{\mathbf{K}^{(1)}_{dd}} & \mathbf{0} \\ \mathbf{0} & \mathbf{0} & \underset{(m-2)\times3}{\mathbf{K}^{(2)}_{dc}} & \underset{(n-2)\times3}{\mathbf{K}^{(2)}_{db}} & \mathbf{0} & \underset{3(n-2)\times3(n-2)}{\mathbf{K}^{(2)}_{dd}} \end{bmatrix}$$

$$= \begin{bmatrix} \underset{12\times12}{\mathbf{K}^{(1\&2)}_{bcb}} & \underset{12\times3(m+n-4)}{\mathbf{K}^{(1\&2)}_{bcd}} \\ \underset{3(m+n-4)\times12}{\mathbf{K}^{(1\&2)}_{dcb}} & \underset{3(m+n-4)\times3(m+n-4)}{\mathbf{K}^{(1\&2)}_{ddd}} \end{bmatrix}, \tag{30}$$

while the mass matrix takes the form

$$\mathbf{M} = \begin{bmatrix} \underset{12\times12}{\mathbf{0}} & \underset{12\times3(m-2)}{\mathbf{0}} & \underset{12\times3(n-2)}{\mathbf{0}} \\ \underset{3(m-2)\times12}{\mathbf{0}} & \underset{3(m-2)\times3(m-2)}{\mathbf{M}^{(1)}_{dd}} & \underset{3(m-2)\times3(n-2)}{\mathbf{0}} \\ \underset{3(n-2)\times12}{\mathbf{0}} & \underset{3(n-2)\times3(m-2)}{\mathbf{0}} & \underset{3(n-2)\times3(n-2)}{\mathbf{M}^{(2)}_{dd}} \end{bmatrix} = \begin{bmatrix} \underset{12\times12}{\mathbf{0}} & \underset{12\times3(m+n-4)}{\mathbf{0}} \\ \underset{3(m+n-4)\times12}{\mathbf{0}} & \underset{3(m+n-4)\times3(m+n-4)}{\mathbf{M}^{(1\&2)}_{ddd}} \end{bmatrix}, \tag{31}$$

and the nodal degrees of freedom are grouped in the algebraic vector:

$$\boldsymbol{\delta}^{\mathrm{T}} = \begin{bmatrix} \underset{1\times3}{\boldsymbol{\delta}^{(1)}_{bb}} & \underset{1\times3}{\boldsymbol{\delta}^{(1)}_{cc}} & \underset{1\times3}{\boldsymbol{\delta}^{(2)}_{cc}} & \underset{1\times3}{\boldsymbol{\delta}^{(2)}_{bb}} & \underset{1\times3(m-2)}{\boldsymbol{\delta}^{(1)}_{dd}} & \underset{1\times3(n-2)}{\boldsymbol{\delta}^{(2)}_{dd}} \end{bmatrix} = \begin{bmatrix} \underset{1\times12}{\boldsymbol{\delta}^{(1\&2)}_{bcb}} & \underset{1\times3(m+n-4)}{\boldsymbol{\delta}^{(1\&2)}_{ddd}} \end{bmatrix}^{\mathrm{T}}. \tag{32}$$

In the above matrices and vector, the partitioning due to domain decomposition is set forth by subscripts *b*, *c*, *d*, referring to the system dof and standing for *boundary*, *crack* and *domain*, respectively, while the apices $^{(1)}$ and $^{(2)}$ refer to the arch segments composing the damaged structure. In order to make the computation more efficient, the kinematic condensation of *non-domain* (boundary and crack) dof is performed

$$\{\mathbf{K}^{(1\&2)}_{ddd} - \mathbf{K}^{(1\&2)}_{dcb}[\mathbf{K}^{(1\&2)}_{bcb}]^{-1}\mathbf{K}^{(1\&2)}_{bcb}\}\boldsymbol{\delta}^{(1\&2)}_{ddd} = \omega^2\mathbf{M}^{(1\&2)}_{ddd}\boldsymbol{\delta}^{(1\&2)}_{ddd}. \tag{33}$$

Table 1
Physical parameters used in the analysis of free vibrations of the uniform arch

Parameter	Value
Density of mass, ρ	$7860\,\mathrm{kg/m^3}$
Young's modulus, E	210,000 MPa
Shear modulus, G	80,770 MPa
Arch radius, R	1.0 m
Opening angle, 2Θ	100°
Cross section area, A	$4.8\times10^{-3}\,\mathrm{m^2}$
Moment of inertia, I	$2.56\times10^{-6}\,\mathrm{m^4}$
Shear factor, χ	1.2

The natural frequencies of the structure considered can be determined by vanishing the determinant:

$$|\{\mathbf{K}^{(1\&2)}_{ddd}-\mathbf{K}^{(1\&2)}_{dcb}[\mathbf{K}^{(1\&2)}_{bcb}]^{-1}\mathbf{K}^{(1\&2)}_{bcd}\}-\omega^2\mathbf{M}^{(1\&2)}_{ddd}|=0. \tag{34}$$

4. Applications

In the present paragraph, some results and considerations about the free vibration problem of both undamaged and damaged circular arches, with different boundary conditions are presented. The analysis has been carried out by means of the analytical and numerical procedures enlightened before.

The aims of this study are to emphasize how the modal parameters vary with the damage level and cracking location and also to validate the reliability of the numerical approach, when a large number of natural frequencies need to be evaluated.

In the following, numerical results related to two different circular arches, whose geometrical and mechanical characteristics are listed in Table 1, are presented; the first one showing clamped–clamped end conditions [34], the second one hinged–hinged. In particular, three damage locations, $\theta_1^*=-10^\circ$, $\theta_2^*=-30^\circ$, $\theta_3^*=-40^\circ$, for two damage levels D_1 and D_2 (corresponding to $K_1=10EI/R$ and $K_2=EI/R$, respectively) have been considered in detail.

Tables 2 and 3 show the first ten eigenfrequencies, in Hz, corresponding to the two considered arches, comparing the solutions of the two methods.

It is evident how the D.Q. technique produces practically coincident results, when compared with analytical ones, using only a few sampling points along the two subdomains, for all the cases examined. It is to be noted, however, that, when passing from undamaged configurations to damaged ones, for the first four modes, only a few more grid points are needed, to compute the correct eigenparameters (see Figs. 2 and 3); while almost a double number of grid nodes needs to be used in order to obtain the same accuracy for higher modes. One remarkable feature, comparing the two approaches, is that the computational cost decreases significantly using the D.Q. procedure and this might be of interest when plotting frequency variations versus damage

Table 2
Comparison between theoretical and numerical frequencies for a uniform clamped–clamped circular arch

Mode	Undamaged (a)			Damage D_1 (b)			Damage D_2 (c)		
	Exact (Hz)	GDQ (Hz)	Error (%)	Exact (Hz)	GDQ (Hz)	Error (%)	Exact (Hz)	GDQ (Hz)	Error (%)
(1)									
1	328.2	328.2	0.0	321.4	321.3	0.0	295.1	295.0	0.0
2	546.6	546.6	0.0	540.6	540.3	0.0	520.9	520.7	0.0
3	854.1	854.1	0.0	852.0	852.4	0.1	838.8	838.9	0.0
4	1078.5	1078.5	0.0	1037.1	1041.1	0.4	939.8	944.3	0.5
5	1642.0	1642.0	0.0	1636.0	1641.7	0.3	1612.2	1619.3	0.4
6	1646.3	1646.3	0.0	1642.9	1643.9	0.1	1642.6	1643.8	0.1
7	2240.2	2240.3	0.0	2177.8	2207.9	1.4	2047.9	2069.8	1.1
8	2813.9	2814.0	0.0	2777.2	2874.7	3.5	2716.3	2816.9	3.7
(2)									
1	328.2	328.2	0.0	323.3	323.3	0.0	302.7	302.7	0.0
2	546.6	546.6	0.0	533.7	533.7	0.0	493.3	493.3	0.0
3	854.1	854.1	0.0	842.3	842.3	0.0	806.9	806.9	0.0
4	1078.5	1078.5	0.0	1055.4	1055.4	0.0	1010.6	1010.6	0.0
5	1642.0	1642.0	0.0	1626.2	1626.3	0.0	1588.5	1588.6	0.0
6	1646.3	1646.3	0.0	1644.4	1644.5	0.0	1644.3	1644.3	0.0
7	2240.2	2240.3	0.0	2236.7	2236.8	0.0	2225.9	2225.9	0.0
8	2813.9	2814.0	0.0	2751.4	2752.9	0.1	2592.6	2592.6	0.1
(3)									
1	328.2	328.2	0.0	326.6	326.6	0.0	322.0	321.9	0.0
2	546.6	546.6	0.0	544.6	544.4	0.0	539.2	539.2	0.0
3	854.1	854.1	0.0	853.4	853.4	0.0	850.8	850.8	0.0
4	1078.5	1078.5	0.0	1068.6	1068.6	0.0	1039.1	1039.1	0.0
5	1642.0	1642.0	0.0	1610.0	1610.3	0.0	1520.4	1520.8	0.0
6	1646.3	1646.3	0.0	1646.2	1646.2	0.0	1646.2	1646.2	0.0
7	2240.2	2240.3	0.0	2182.6	2184.4	0.1	2063.8	2064.9	0.1
8	2813.9	2814.0	0.0	2755.8	2754.4	−0.1	2664.9	2660.8	−0.2

Angular coordinate of the damage: (1) $\theta_1^* = -10^\circ$, (2) $\theta_2^* = -30^\circ$, (3) $\theta_3^* = -40^\circ$. Stiffness of the spring: (a) $K \to \infty$; (b) $K = 10EI/R$; (c) $K = EI/R$. Collocations adopted: (1) $m = 11$, $n = 11$; (2) $m = 11$, $n = 15$; (3) $m = 9$, $n = 17$.

locations and intensities. The D.Q. approximation proposed (Lagrange interpolation), using the domain decomposition technique, is sufficiently accurate for the cases treated, since no steep variation of dependent variables (displacements) is expected in the interior of the domain(s), but only in the vicinity of boundaries, or cracked sections.

Figs. 4 and 5 represent the first six modal shapes, for both undamaged and damaged configurations. For what concerns the undamaged reference configuration (dotted line), the even and odd modes are, respectively, symmetric and skew-symmetric with respect to the middle section of the arch. The sixth modal shape of the hinged arch shows a different behavior, when

Table 3
Comparison between theoretical and numerical frequencies for a uniform hinged–hinged circular arch

Mode	Undamaged (a)			Damage D_1 (b)			Damage D_2 (c)		
	Exact (Hz)	GDQ (Hz)	Error (%)	Exact (Hz)	GDQ (Hz)	Error (%)	Exact (Hz)	GDQ (Hz)	Error (%)
(1)									
1	201.5	201.4	0.0	198.1	198.1	0.0	184.0	184.0	0.0
2	460.7	460.7	0.0	452.7	452.7	0.0	422.9	422.9	0.0
3	801.2	801.2	0.0	800.1	800.1	0.0	757.2	757.2	0.0
4	886.5	886.5	0.0	852.9	852.9	0.0	805.9	805.9	0.0
5	1400.3	1400.3	0.0	1400.3	1400.3	0.0	1400.3	1400.3	0.0
6	1646.3	1646.3	0.0	1637.1	1637.1	0.0	1600.2	1600.2	0.0
7	1985.4	1985.4	0.0	1924.8	1924.8	0.0	1808.5	1808.5	0.0
8	2575.3	2575.3	0.0	2545.8	2545.8	0.0	2494.5	2494.4	0.0
(2)									
1	201.5	201.4	0.0	192.1	192.1	0.0	150.9	150.9	0.0
2	460.7	460.7	0.0	445.4	445.4	0.0	402.6	402.6	0.0
3	801.2	801.2	0.0	795.4	795.4	0.0	775.8	775.8	0.0
4	886.5	886.5	0.0	876.3	876.3	0.0	857.7	857.7	0.0
5	1400.3	1400.3	0.0	1400.3	1400.3	0.0	1400.3	1400.3	0.0
6	1646.3	1646.3	0.0	1636.6	1636.6	0.0	1603.2	1603.2	0.0
7	1985.4	1985.4	0.0	1963.5	1963.5	0.0	1897.5	1897.5	0.0
8	2575.3	2575.3	0.0	2490.3	2490.2	0.0	2324.1	2323.9	0.0
(3)									
1	201.5	201.4	0.0	197.4	197.4	0.0	168.5	168.5	0.0
2	460.7	460.7	0.0	445.7	445.7	0.0	374.9	374.9	0.0
3	801.2	801.2	0.0	800.4	800.4	0.0	733.0	733.0	0.0
4	886.5	886.5	0.0	850.2	850.2	0.0	803.5	803.5	0.0
5	1400.3	1400.3	0.0	1344.8	1344.8	0.0	1232.4	1232.4	0.0
6	1646.3	1646.3	0.0	1645.5	1645.5	0.0	1644.0	1644.0	0.0
7	1985.4	1985.4	0.0	1925.1	1925.0	0.0	1834.0	1833.9	0.0
8	2575.3	2575.3	0.0	2528.3	2529.2	0.0	2467.5	2468.4	0.0

Angular coordinate of the damage: (1) $\theta_1^* = -10^\circ$, (2) $\theta_2^* = -30^\circ$, (3) $\theta_3^* = -40^\circ$. Stiffness of the spring: (a) $K \to \infty$; (b) $K = 10EI/R$; (c) $K = EI/R$. Collocations adopted: (1) $m = 11$, $n = 11$; (2) $m = 11$, $n = 15$; (3) $m = 9$, $n = 17$.

compared to the others; in fact, the principal displacement component is the radial one, while practically null tangential translation occurs (prevalent axial mode).

In the damaged cases (dashed and solid lines), mode shapes show no symmetry/skew-symmetry anymore and generally differ from the undamaged ones. It is to be noted, however, that, for the lightest damage level configuration (D_1), no major differences are encountered when a comparison is made with the corresponding undamaged case.

With regard of the frequencies variations, as expected, they show to be dependent on both crack position and damage severity, as one can infer from Tables 2 and 3. A parametric study has been conducted, to investigate the behavior of the damaged arch, when the crack location varies along

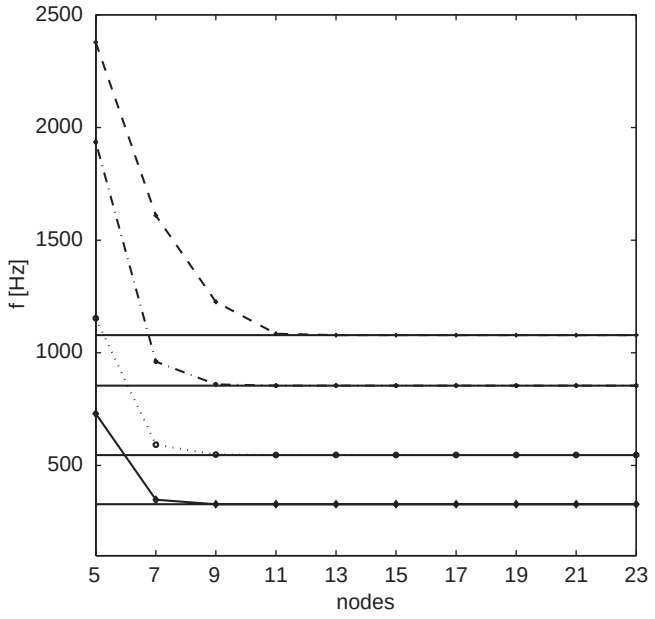

Fig. 2. Convergence characteristics of clamped–clamped undamaged arch for the first four frequencies, by comparison with analytical results.

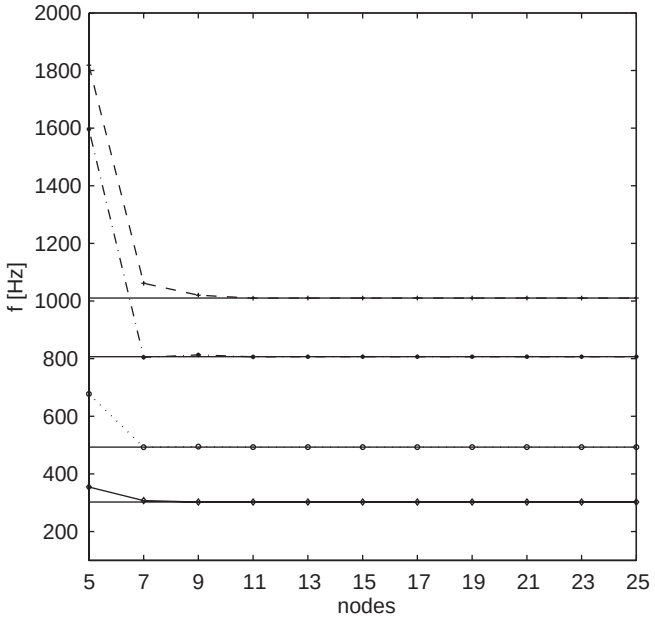

Fig. 3. Convergence characteristics of clamped–clamped damaged arch for the first four frequencies, by comparison with analytical results. Angular coordinate of the cracked cross section: $\theta_1^* = -30^\circ$, damage configuration D_2.

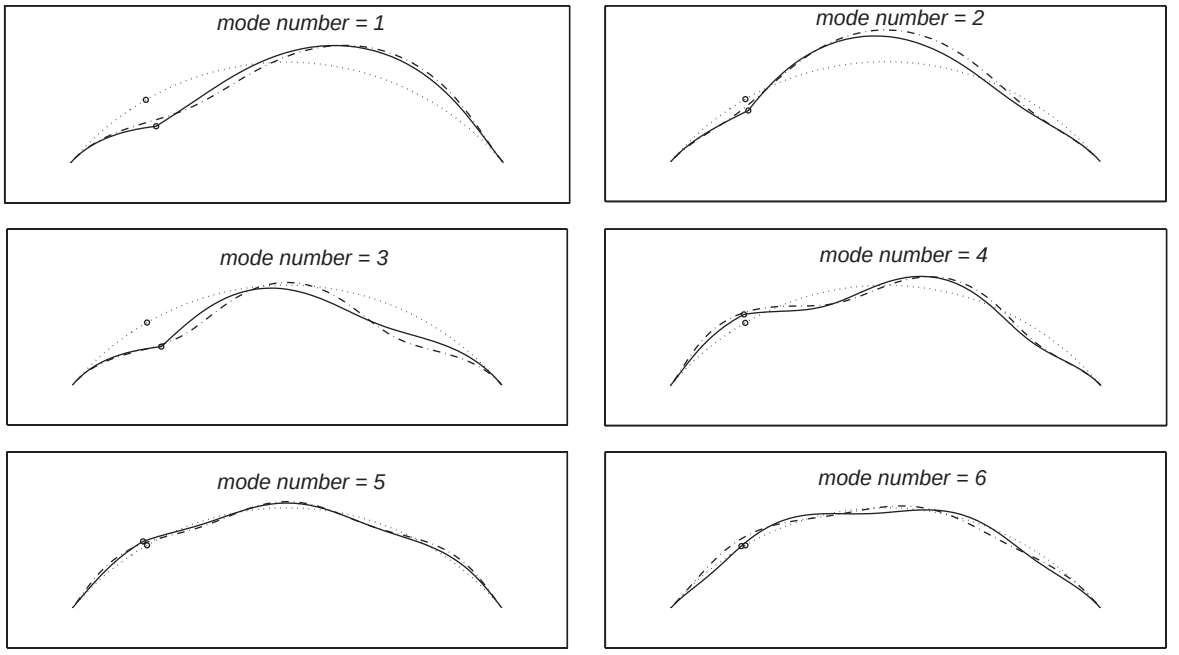

Fig. 4. Modal shapes relative to the free vibrations of the clamped–clamped circular arch in undamaged and damage configuration D_2. Angular coordinate of the cracked cross section: $\theta_1^* = -30^\circ$.

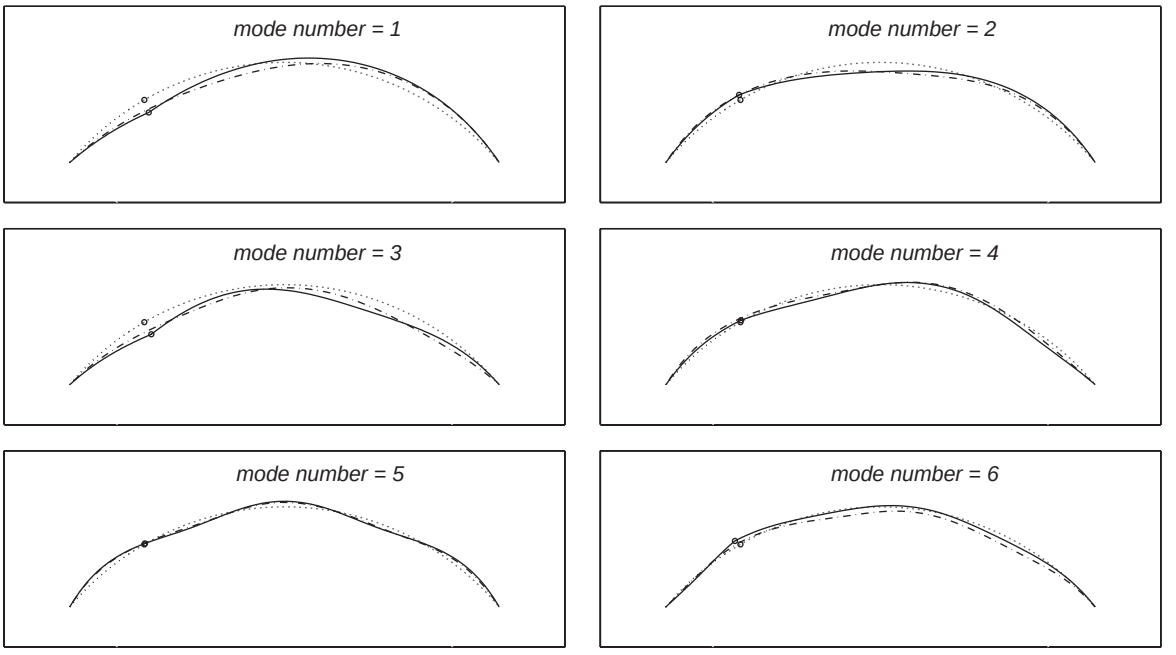

Fig. 5. Modal shapes relative to the free vibrations of the hinged–hinged circular arch in undamaged and damage configuration D_2. Angular coordinate of the cracked cross section: $\theta_1^* = -30^\circ$.

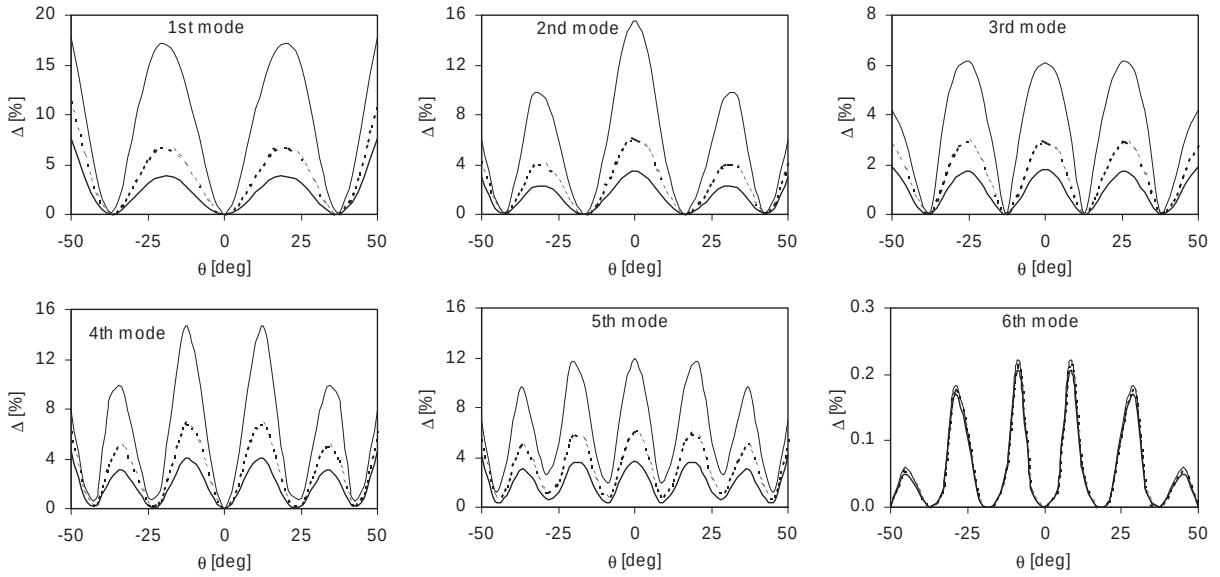

Fig. 6. Frequency relative variations of the clamped–clamped circular arch versus damage location θ, for different levels of damage severity. Solid thick line: $K = 10EI/R$; dashed thick line: $K = 5EI/R$; solid thin line: $K = EI/R$.

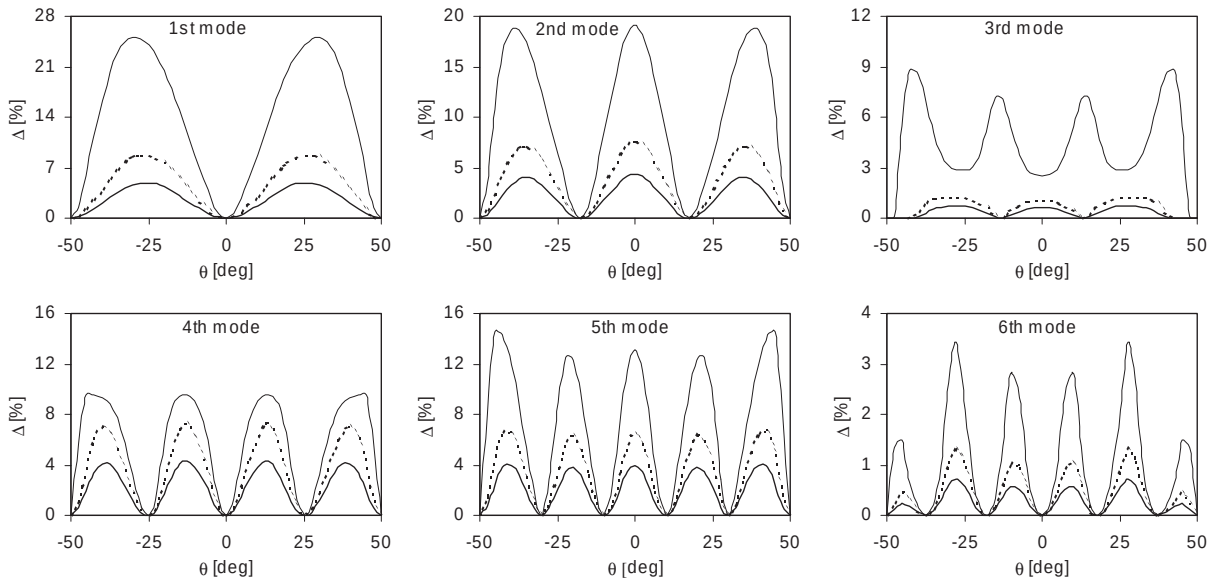

Fig. 7. Frequency relative variations of the hinged–hinged circular arch versus damage location θ, for different levels of damage severity. Solid thick line: $K = 10EI/R$; dashed thick line: $K = 5EI/R$; solid thin line: $K = EI/R$.

the axis and for different levels of damage. Figs. 6 and 7 show the frequency relative variations curves, for the first six modes of both clamped and hinged arches. As expected, the frequency variations increase with the damage severity, i.e. as the elastic stiffness K decreases. On the other hand, for a fixed value of K, the frequency variations depend on the crack position along the arch. It is worth noting that frequency variations are symmetric with respect to the middle section and that different damage locations can give rise to the same variations. This fact must be taken into account, when a cracking position estimate by modal parameters measures is performed, in a way that different crack locations, for a given damage severity, can correspond to the same measured frequency.

5. Conclusions

In this paper, two different approaches to the study of free harmonic in-plane vibration of circular arches have been presented. Both undamaged and damaged configurations have been explored, modeling the cracked section as an elastic rotational spring. Both methods show accurate in predicting natural frequencies and useful in plotting mode shapes and can be conveniently adopted in localizing a cracked section by modal parameters measures. As a future address, it could be interesting to compare the analytical frequencies and modal shapes estimates with experimentally measured ones. A possible further extension, in the numerical range, could be the taking into account of structural nonlinearity and a more refined theoretical modeling of the crack.

References

[1] H. Lamb, On the flexure and the vibration of a curved bar, *Proceedings of the London Mathematical Society* 19 (1888) 365–376.
[2] A.E.H. Love, *A Treatise on the Mathematical Theory of the Elasticity*, Dover, New York, 1944.
[3] J.P. Den Hartog, The lowest natural frequency of circular arcs, *Philosophical Magazine Series 7* 5 (1928) 400–408.
[4] X. Tong, N. Mrad, B. Tabarrok, In-plane vibrations of circular arches with variable cross-sections, *Journal of Sound and Vibration* 212 (1988) 121–140.
[5] N.M. Auciello, M.A. De Rosa, Free vibrations of circular arches: a review, *Journal of Sound and Vibration* 176 (1994) 433–458.
[6] P. Chidamparam, W. Leissa, Influence of centerline extensibility on the in-plane free vibrations of loaded circular arches, *Journal of Sound and Vibration* 183 (1995) 779–795.
[7] K. Kang, C.W. Bert, A.G. Striz, Vibration and buckling analysis of circular arches using DQM, *Computers & Structures* 60 (1996) 49–57.
[8] E. Tüfekçi, A. Arpaci, Exact solution of in-plane vibrations of circular arches with account taken of axial extension, transverse shear and rotatory inertia, *Journal of Sound and Vibration* 209 (1998) 845–856.
[9] J.-S. Wu, L.-K. Chiang, Free vibration analysis of arches using curved beam elements, *International Journal for Numerical Methods in Engineering* 58 (2003) 1907–1936.
[10] T. Irie, G. Yamada, K. Tanaka, Natural frequencies of in-plane vibration of arcs, *Journal of Applied Mechanics* 50 (1983) 449–452.
[11] A. Benedetti, L. Deseri, A. Tralli, Simple and effective equilibrium models for vibration analysis of curved rods, *Journal of Engineering Mechanics* 122 (1996) 291–299.

[12] Y.P. Tseng, C.S. Huang, C.J. Lin, Dynamic stiffness analysis for in-plane vibrations of arches with variable curvature, *Journal of Sound and Vibration* 207 (1997) 15–31.
[13] P.F. Rizos, N. Aspragathos, A.D. Dimarogonas, Identification of crack location and magnitude in a cantilever beam from the vibration modes, *Journal of Sound and Vibration* 138 (1990) 381–388.
[14] W.M. Ostachowicz, M. Krawczuk, Analysis of the effect of a crack on the natural frequencies of a cantilever beam, *Journal of Sound and Vibration* 150 (1991) 191–201.
[15] M.N. Cerri, G.C. Ruta, Detection of localised damage in plane circular arches by frequency data, *Journal of Sound and Vibration* 270 (2004) 39–59.
[16] M.H.H. Shen, J.E. Taylor, An identification problem for vibrating cracked beam, *Journal of Sound and Vibration* 150 (1991) 457–484.
[17] M. Krawczuk, W.M. Ostachowicz, Natural vibrations of a clamped–clamped arch with an open transverse crack, *Journal of Vibration and Acoustics* 119 (1997) 145–151.
[18] L.B. Freund, G. Herrmann, Dynamic fracture of a beam or plate in plane bending, *Journal of Applied Mechanics* 76-APM-15 (1976) 112–116.
[19] E. Cabib, L. Freddi, A. Morassi, D. Percivale, Thin notched beams, *Journal of Elasticity* 64 (2001) 157–178.
[20] E. Viola, L. Federici, L. Nobile, Detection of crack location using cracked beam element method for structural analysis, *Theoretical and Applied Fracture Mechanics* 36 (2001) 23–35.
[21] E. Viola, L. Nobile, L. Federici, Formulation of crack beam element method for structural analysis, *Journal of Engineering Mechanics* 128 (2002) 220–230.
[22] C.W. Bert, M. Malik, Differential quadrature method in computational mechanics: a review, *Transactions of the American Society of Mechanical Engineers* 49 (1996) 1–28.
[23] K. Kang, C.W. Bert, A.G. Striz, Vibration analysis of shear deformable circular arches by the differential quadrature method, *Journal of Sound and Vibration* 181 (1995) 353–360.
[24] K. Kang, C.W. Bert, A.G. Striz, Vibration and buckling analysis of circular arches using DQM, *Computers & Structures* 60 (1) (1996) 49–57.
[25] T.Y. Wu, G.R. Liu, Y.Y. Wang, Application of the generalized differential quadrature rule to initial-boundary-value problems, *Journal of Sound and Vibration* 264 (2003) 883–891.
[26] G.R. Liu, T.Y. Wu, In-plane vibration analysis of circular arches by the generalized differential quadrature rule, *International Journal of Mechanical Sciences* 43 (11) (2003) 2597–2611.
[27] G.R. Liu, T.Y. Wu, Vibration analysis of beams using the generalized differential quadrature rule and domain decomposition, *Journal of Sound and Vibration* 246 (2001) 461–481.
[28] M.A. De Rosa, C. Franciosi, Non-classical boundary conditions and DQM, *Journal of Sound and Vibration* 214 (1998) 743–748.
[29] N. Bellomo, Nonlinear models and problems in applied sciences from differential quadrature to generalized collocation methods, *Mathematical Computation and Modelling* 4 (1997) 13–34.
[30] A.S. Veletsos, W.J. Austin, C.A. Lopes Pereira, W. Shyr-Jen, Free vibration of circular arches, *Journal of Engineering Mechanics Division* 98 (1972) 311–329.
[31] A.D. Dimarogonas, S.A. Paipetis, *Analytical Methods in Rotor Dynamics*, Applied Science, London, 1983.
[32] N. Bellomo, L. Preziosi, *Modelling*, *Mathematical Methods and Scientific Computation*, CRC Press, Boca Raton, FL, 1995.
[33] C. Shu, W. Chen, On optimal selection of interior points for applying discretized boundary conditions in DQ vibration analysis of beams and plates, *Journal of Sound and Vibration* 222 (1999) 239–257.
[34] M. Santoni, Analisi Dinamica degli Archi con Elementi Finiti Misti, Thesis University of Bologna, Italy, 2001 (in Italian).